DOI: 10.61782/fa.2023.1023

forum acusticum 2023

SOLAR PHOTOVOLTAIC MODULE DEFECT EVALUATION WITH HIGHER ORDER MODES OF LAMB WAVES

Dicky Silitonga[1*] **Nico F. Declercq**[1]
[1] G.W. Woodruff School of Mechanical Engineering, IRL 2958 Georgia Tech-CNRS, Metz, France

ABSTRACT

In the growing solar photovoltaic (PV) power generation sector, PV modules' quality assurance and structural integrity are indispensable parts of production and maintenance activities that ensure the power plant delivers optimum performance throughout its expected lifetime. Therefore, proper inspections should be carried out during the manufacturing process and operation. Ultrasonics offers advantages in mechanical defect detection compared to other electronic-based methods focusing on cells and circuitry faults. Among the known ultrasonic techniques, the one based on guided waves, particularly Lamb waves, shows a promising potential for large-scale inspection of solar PV modules, owing to its ability to cover long-range and hence faster measurement. Conventionally, Lamb waves investigation exploits the fundamental modes in the non-dispersive regime. However, that approach is not always effective for all cases, including in the PV module we investigate, since the modes may not be sensitive to certain defect types. This work demonstrates that higher-order modes are more helpful in inspecting defective solar modules since they have better damage sensitivity. Moreover, these modes are not necessarily to be excited in their non-dispersive regime for damage identification purposes, thus reducing complexity in determining the excitation signal parameters.

Keywords: *Solar cells, Non-destructive testing, Ultrasonics, Lamb waves*

[*] ***Corresponding author***: *dsilitonga@gatech.edu or djsilitonga@gmail.com.*

1. INTRODUCTION

Solar PV is becoming increasingly favored as a green and sustainable option for electricity generation. Continuous improvements in efficiency and cost-effectiveness lead to a broad exposure of this technology not only for the utility-scale grid supplier but also for the small, decentralized power plants. However, as with any material, solar PV modules may contain defects initiated during manufacturing and handling or developed over time as they operate. In the production stage, defects, such as cracks, are intolerable since they cannot be repaired and will severely impact the module's efficiency and lifetime. Therefore, properly inspecting the manufacturing line is imperative to avoid defective products being delivered to the market.

This paper focuses on a defect in the form of a crack in the front glass of a solar module. Glass crack or breakage is a crucial failure mode since its presence will accelerate module degradation by permitting moisture ingress that leads to the deterioration of cells and electrical conductor lines [1]. Cracks are usually examined in the quality control procedure with visual inspection [2,3]. Despite its simplicity, the manual process has disadvantages, such as time consumption and subjectivity of inspection results, since it relies on human perception. Other methods exist: ultrasonic C-scan, a mature non-destructive testing (NDT) method widely implemented on various materials. Still, the method has a significant drawback in that it requires a considerable amount of time to make a scan, hence inappropriate for a fast-moving, mass-production process.

In this work, another ultrasonic method is proposed for the NDT of solar modules, employing Lamb waves as the damage detector. The main advantage of Lamb waves is their long propagation range, which allows a large area to be inspected at once. Consequently, measurement time will be significantly shortened compared to the conventional C-scan. This work is built upon the findings of a previous investigation [4] which discovers a high-order Lamb mode sensitive to crack. According to the experiments and

numerical results, four Lamb modes are excited in the solar module specimen examined in the research, namely modes 1, 2, 5, and 11. Out of those propagating modes, only the high order, mode 11, is exceptionally sensitive to the crack in the front glass of the solar panel. With that knowledge, a scanning method based on Lamb waves is developed to detect cracks as an automated module inspection intended for a quality control system.

2. METHODS

The technique uses a pair of transducers in a pitch-catch setup to interrogate a material section between them. A greater spacing is preferred because a wider area can be covered in a single measurement. However, increasing the distance will lead to a loss of signal energy due to attenuation. Thus, finding the appropriate transducer spacing that will provide a good balance between those two aspects is essential. In this study, a distance of 50 mm distance is taken.

During the measurement, a pulse of sinusoidal 500 kHz signal from a waveform generator (Stanford Research Systems DS345) is sent through an amplifier (Krohn-Hite 7500, 10x gain) to the emitter (Olympus V103) that is held on a frame together with the receiver of the same transducer model. Both transducers contact the solar module's front glass surface at a normal incidence angle, with water as the coupling. To make a scan, the transducers are driven by the arm of the 5-axis ultrasonic scanner (TransformNDT-ITE Polar C-Scan). The setup is illustrated in Figure 1.

For each position of the transducer pair, the emitter excites Lamb waves in the solar module structure that are captured on the receiver's side. Thus, the captured signal contains information on the structural condition in the waves' straight line path from the emitter to the receiver. With this setup, each line scan stroke will inspect an area enclosed by a rectangle with a width equal to the transducers' spacing (50 mm) and a length equal to the scanning travel distance. In other words, a single line scan with this method will evaluate a particular area, in contrast to the conventional C-scan, where multiple strokes are required to evaluate that area.

The specimen is a thin-film tandem (amorphous and microcrystalline silicon) solar module. Three sections of the solar module area are measured to represent different structural health conditions, as shown in Figure 2. As shown in Figure 2 (a) and (b), measurements on pristine and fully cracked sections will reference the undamaged and defective conditions. Then, a measurement on a partially cracked section, depicted in Figure 2 (c), demonstrates the case where there are transitions from one condition to another. The measurement is made by performing a line scan of 100 mm with a resolution of 1 mm.

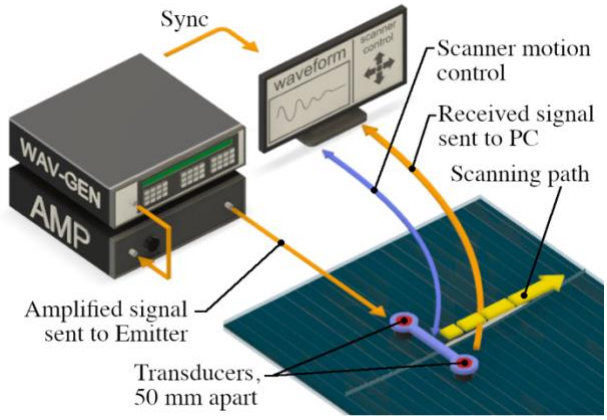

Figure 1. Schematic of the experiment: two transducers are held 50 mm apart, dragged by the scanner arm following a line path.

Signal analysis is performed in the frequency domain since time domain parameters depend highly on the physical circumstances during measurement. The commonly used approach of velocity change analysis is unsuitable for randomly located defects since the time of arrival of a signal passing through defects will vary depending on the position of the defects relative to the transducers. Frequency domain analysis, however, is more reliable because although random variations exist in the signal's arrival time, the frequency content of the signal and the proportion in the spectrum remain consistent.

Based on the finding that the high order mode (mode 11) is sensitive to crack, the main idea of this technique is to quantify the proportion of this mode in the spectrum. The calculated proportion is in terms of energy spectrum density (ESD), where the ESD of a given bandwidth is given by Equation 1 as written in the Equation part at the end of this paper. Then, the proportion of the ESD of mode 11 is obtained as the ratio of ESD in the range where the mode lies (1000 kHz – 1200 kHz) and the ESD of the whole spectrum to include all propagating modes (50 kHz – 1200 kHz). The ratio, as expressed by Equation 2, is then plotted for all points along the scanning length to reveal the condition of the inspected area.

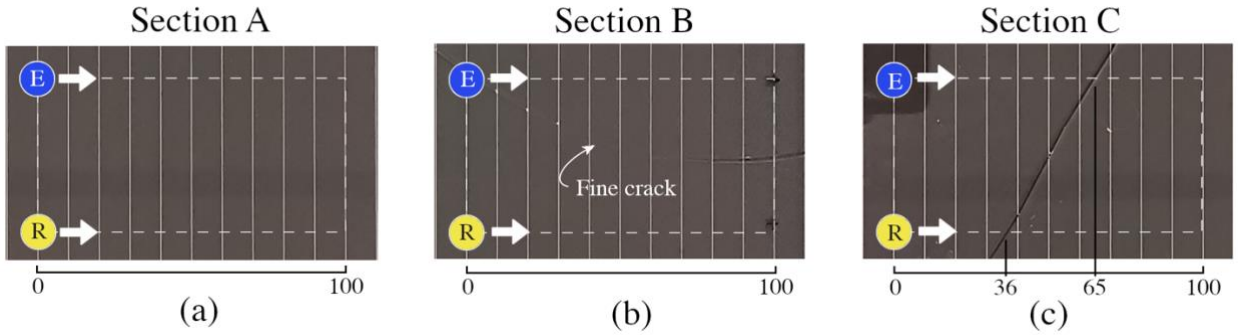

Figure 2. The sections measured in the experiments cover an area of 50 mm (distance between transducers) by 100 mm (scanning length). (a) Pristine section; (b) Section with a crack along the scanning length; (c) Section with partial crack: when the scanner moves following the direction of the arrow, the receiver (R) encounters the crack first at 36 mm and then the emitter (E) at 65 mm. The diameter of the transducer is 15 mm.

3. RESULTS AND DISCUSSION

The typical frequency spectrum of the Lamb waves propagating in the structure over the pristine area is plotted in Figure 3. The peaks in that Fourier space are per the frequency bands where propagating modes appear in the dispersion curves of this solar module, as elaborated in reference [4]. Per the referenced paper, those four significant peaks belong to modes 1, 2, 5, and 11. Mode 11 is the highest order mode where, in this investigation, the frequency band considered for analysis is from 1000 kHz to 1200 kHz, as indicated in the figure.

As stated earlier in the previous section, the proportion of ESD of mode 11 in the spectrum is utilized as a damage indicator. When there is a discontinuity in the Lamb waves' propagation path, in this case, a crack, the energy density in the frequency band containing mode 11 will decrease, reducing its significance in the spectrum.

The ESD proportion of mode 11 for all three measured sections is plotted in Figure 4, expressed as a percentage of the spectrum ESD for each point throughout the 100 mm scanning length. Although the percentage levels fluctuate over the scanning length, the data points of measurement results of area A are always above those from area B, demonstrating the capability of this method to differentiate between pristine and defective structures. Note that the plot of each section represents a set of measurements on 100 points (scanning 100 mm long at 1 mm resolution). Therefore, they can also be considered data sets for statistical purposes, for instance, to describe that the minimum percentage level obtained from 100 measurements on the entire area is 6%. Further, this level can be used as a threshold below which the inspected region is suspected to be defective.

A vital remark from the observation of the measurement result of section B in Figure 4 is that even if the crack is not readily visible with the eyes (see Figure 2(b)), it is detectable with this technique. This fact is evident since the percentage level of section B is below that of section A (undamaged area) at all points. Undoubtedly, it shows the benefit and usefulness of this method over manual visual inspection.

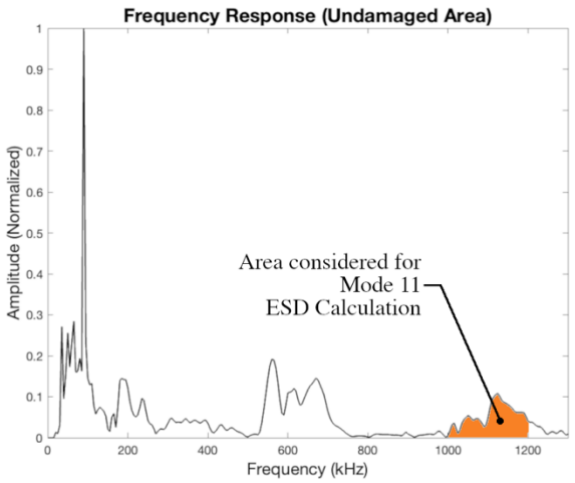

Figure 3. The spectrum of Lamb waves in the undamaged area, where mode 11 is located in the 1000 kHz – 1200 kHz range. The other lower-frequency major peaks are of modes 1, 2, and 5.

Meanwhile, the results from measurements on sections A and B provide the indicative levels that distinguish the pristine and cracked sections; the partially cracked section C allows assessment of the measurement technique in

another realistic case. Lamb wave scan on a partially defective sample has been practiced in numerous research, for example, in the detection of delamination spots [5], impacted part [6], or a hole [7] in a plate structure. Nevertheless, most investigations evaluate samples with artificial defects in the middle of the gap between transducers. This work extends the crack from one transducer scan trajectory line to another. In addition, the crack is in an oblique orientation relative to the transducers' line of sight.

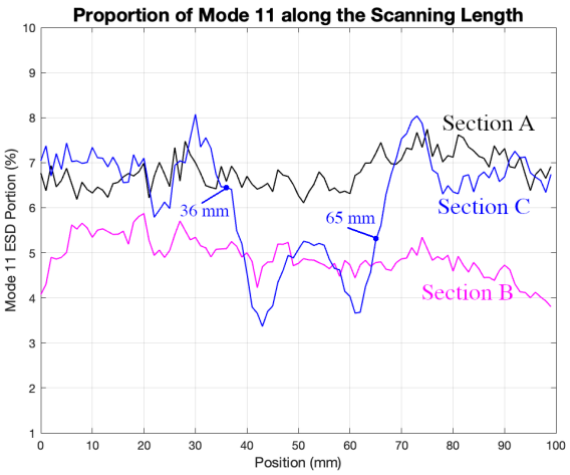

Figure 4. Percentage of ESD portion of mode 11 in the spectrum, obtained from 100 mm scan on 3 sample sections of different conditions. In section C, the physical crack starts at 36 mm and ends at 65 mm (Refer to Figure 2).

The plot of section C in Figure 4 shows that the level drops around the region where there is a crack between the transducers when they pass that region. Physically, during the measurement, the crack appears 36 mm into the scan and clears after 65 mm, as shown in Figure 2(c). However, the points where the level drops/recovers in the plot of section C are not precisely at the entry and exit of the cracked region, which is due to the size of the transducers. The transducers' diameter is 15 mm, so when they pass a crack, it requires that amount of displacement to switch entirely from one side of the cracked region to the adjacent. Hence no sudden transition exists. This issue can be mitigated by using transducers with pointy faces like the one proposed in reference [8].

In the Mode 11 ESD plot of section C, it is also noticeable that the percentage level exhibits a particular manner. The percentage level spikes when a transducer is close to the crack line, and the crack is not between two transducers. That rise in proportion is because the high-frequency part of the waves reflected by the nearby discontinuity still has sufficient energy in the received signal. Meanwhile, when the reflector is far from the transducer, the high-frequency part of reflected waves would have been attenuated during the travel, resulting in an insignificant contribution to the received signal. In short, the effect of reflected waves on the proportion of high-frequency parts only appears when the transducer is close to the crack.

In the transition region where the transducer's diameter covers both sides of the crack line, the level drops deeper, which means the proportion of the high-frequency part of the signal is even lower. It can be due to the improper contact condition of the structure-transducer coupling when a single transducer face induces vibration to two separate structures. Once both transducers clear the crack line, the level rises to the magnitude range around the thoroughly cracked section B.

Nonetheless, to better understand that near-crack line behavior, knowledge of the scattering characteristics of mode 11 is worth pursuing. Different modes may have distinctive scattering characteristics when incident on a discontinuity, as reported in [9]. A mode in high frequency may have either high or low reflection and transmission coefficients. Investigation into this matter is part of the ongoing work to provide a complete understanding of the phenomena, which will help fine-tune the proposed method's effectiveness.

4. CONCLUSION

This paper has described a technique for crack evaluation on solar modules by employing high-order Lamb waves. The proportion of that high-order mode in the spectrum functions as a damage indicator, which effectiveness has been validated through measurements on areas with different structural conditions. The method has also proven its capability of detecting a fine crack barely visible with human eyes. In a practical application, the embodiment of this method may involve wheel probes or air-coupled transducers for more consistent signal acquisition. Furthermore, the system can be integrated into the moving conveyor line as a part of the quality control process in the solar module manufacturing process.

5. EQUATIONS

The energy spectral density of a bandwidth is the calculated by integrating the square of Fourier modulus, *S(f)*, within the bandwidth limits[10].

$$ESD = \int |S(f)|^2 df \quad (1)$$

The proportion of mode 11 is calculated by dividing the ESD of mode 11 (integration limits from 1000 kHz to 1200 kHz) by the ESD of full spectrum from 0 Hz to 120 kHz.

$$Mode\ 11\ Proportion = ESD_{Mode11} / ESD_{full\ spectrum} \quad (2)$$

6. REFERENCES

[1] J. Zhang, Y. Liu, K. Ding, L. Feng, F.U. Hamelmann, X. Chen: "Model Parameter Analysis of Cracked Photovoltaic Module under Outdoor Conditions", in *47th IEEE Photovolt. Spec. Conf. PVSC*, (Calgary, Canada), pp. 2509–2512, 2020.

[2] E. Caamaño, E. Lorenzo, R. Zilles, "Quality control of wide collections of PV modules: lessons learned from the IES experience", *Prog. Photovolt. Res. Appl.* Vol 7, 137–149, 1999.

[3] J. Balzategui, L. Eciolaza, N. Arana-Arexolaleiba, J. Altube, J.-P. Aguerre, I. Legarda-Ereño, A. Apraiz: "Semi-automatic quality inspection of solar cell based on Convolutional Neural Networks", in *24th IEEE Int. Conf. Emerg. Technol. Fact. Autom. ETFA*, (Zaragoza, Spain), pp. 529–535, 2019.

[4] D. Silitonga, N.F. Declercq, P. Pomarède, F. Meraghni, B. Boussert, P. Dubey: "Ultrasonic guided waves interaction with cracks in the front glass of thin-film solar photovoltaic module", *Sol. Energy Mater. Sol. Cells.*, Vol. 251, 112179, 2023.

[5] K.S. Tan, N. Guo, B.S. Wong, C.G. Tui: "Experimental evaluation of delaminations in composite plates by the use of Lamb waves", *Compos. Sci. Technol.*, Vol 53, pp. 77–84, 1995.

[6] N. Toyama, J. Takatsubo: "Lamb wave method for quick inspection of impact-induced delamination in composite laminates", *Compos. Sci. Technol.*, Vol. 64, pp. 1293–1300, 2004.

[7] L. Mallet, B.C. Lee, W.J. Staszewski, F. Scarpa: "Structural health monitoring using scanning laser vibrometry: II. Lamb waves for damage detection", *Smart Mater. Struct.*, Vol. 13, pp. 261, 2004.

[8] M.A.Y. Barakat, A.E.-A.A. El-Wakil, E.H. Hasan: "Modification of ultrasonic transducers to study crack propagation in vinyl polymers, supported by SEM technique", *J. Vinyl Addit. Technol.*, Vol. 29, pp. 84–99, 2023.

[9] Y. Cho, D.D. Hongerholt, J.L. Rose: "Lamb wave scattering analysis for reflector characterization", I*EEE Trans. Ultrason. Ferroelectr. Freq. Control.*, Vol. 44, pp. 44–52, 1997.

[10] B. Boashash: *Time-Frequency Signal Analysis and Processing Second Ed.*Oxford: Academic Press, 2016.